2+1 flavor QCD simulated in the ϵ-regime in different topological sectors

JHEP11(2009)100

(http://iopscience.iop.org/1126-6708/2009/11/100)

Published by IOP Publishing for SISSA

Received: *June 24, 2009*
Revised: *October 26, 2009*
Accepted: *November 2, 2009*
Published: *November 24, 2009*

JHEP11(2009)100

2+1 flavor QCD simulated in the ϵ-regime in different topological sectors

P. Hasenfratz,[a] **D. Hierl,**[b] **V. Maillart,**[a] **F. Niedermayer,**[a] **A. Schäfer,**[b] **C. Weiermann**[a] **and M. Weingart**[a]

[a] *Albert Einstein Center for Fundamental Physics, Institute for Theoretical Physics, University of Bern, Sidlerstrasse 5, CH-3012 Bern, Switzerland*

[b] *Institute for Theoretical Physics, University of Regensburg, Universitatsstrasse 31, D-93040 Regensburg, Germany*

E-mail: Peter.Hasenfratz@itp.unibe.ch, Dieter.Hierl@physik.uni-regensburg.de, Vidushi.Maillart@itp.unibe.ch, Andreas.Schaefer@physik.uni-regensburg.de, Ferenc.Niedermayer@itp.unibe.ch, Christoph.Weiermann@itp.unibe.ch, Manuel.Weingart@itp.unibe.ch

Abstract: We generated configurations with the parametrized fixed-point Dirac operator $D_{\rm FP}$ on a $(1.6\,\mathrm{fm})^4$ box at a lattice spacing $a = 0.13\,\mathrm{fm}$. We compare the distributions of the three lowest $k = 1, 2, 3$ eigenvalues in the $\nu = 0, 1, 2$ topological sectors with that of the Random Matrix Theory predictions. The ratios of expectation values of the lowest eigenvalues and the cumulative eigenvalue distributions are studied for all combinations of k and ν. After including the finite size correction from NL order chiral perturbation theory we obtained for the chiral condensate in the $\overline{\rm MS}$ scheme $[\Sigma(2\,\mathrm{GeV})]^{1/3} = 0.239(12)\,\mathrm{GeV}$, where the error is statistical only.

Keywords: Lattice QCD, QCD, Chiral Lagrangians

ArXiv ePrint: 0707.0071

doi:10.1088/1126-6708/2009/11/100

Spontaneous chiral symmetry breaking and the related existence of light Goldstone bosons is a basic feature of QCD. Chiral Perturbation Theory (ChPT) provides a systematic description of this physics in terms of a set of low energy constants which encode the related non-perturbative features of QCD. The method of low energy effective Lagrangians simplifies the calculations significantly [1–4] and over the years ChPT became a refined powerful technique. Gasser and Leutwyler recognized very early, decades before the numerical calculations could attack such problems, that these constants can also be fixed using physical quantities which, presumably, will never be measured in real experiments. They can be studied, however, in lattice QCD.

The ϵ- regime [5–8] describes physics close to the chiral limit in a box whose size is larger than the QCD scale. On the other hand, the size of the box relative to the Goldstone boson correlation length must be small. Under these conditions the Goldstone bosons, as opposed to other excitations, feel the effect of boundaries strongly. ChPT provides a powerful and systematic way to calculate the finite size corrections. A nice additional feature of the ϵ-regime is that Random Matrix Theory (RMT) [9] makes precise predictions for microscopic observables. RMT relates in particular the distribution of low-lying eigenvalues of the Dirac operator in different topological sectors to the chiral condensate.

The pioneering numerical works [10–16] in the ϵ-regime in *quenched* QCD suggested that this regime can be an excellent tool to study low-energy physics in QCD. The special problems of the ϵ-regime called for new numerical procedures [14–17] which were first tested also in this approximation. Combining these numerical developments with the renormalization properties of the spectral density the work [18] present a state of the art analysis for the quark condensate and the first Leutwyler-Smilga sum rule in quenched QCD. The quenched approximation, however, tends to be singular in the chiral limit and it is expected that quenching is even more problematic here than in other cases [19].

Unfortunately, full QCD simulations are expensive. In addition, in the $\epsilon-$regime the Dirac operator should have excellent chiral properties. The standard choice is the overlap Dirac operator [20] with a hybrid Monte Carlo algorithm.

The results in [21] reflect already the basic physics features of the ϵ-regime. The distribution of the low-lying eigenmodes could be fitted quite well to the RMT predictions and a reasonable value for the chiral condensate was obtained. These results are promising given the fact that the box was small (1.3 fm), the quark mass was rather large ($m_q \geq 40\,\mathrm{MeV}$) and the lattice was coarse ($a = 0.16\,\mathrm{fm}$). The results in a larger box of 1.5 fm and at smaller quark mass $m_q \approx 20\,\mathrm{MeV}$ obtained in [22] were consistent with those of [21].

The first serious simulation results in the ϵ-regime have been presented by the JLQCD group recently [23]. In that work $N_f = 2$ QCD was simulated with overlap fermions (created with the Wilson kernel) on a lattice of size $1.8^3 \times 3.6\,\mathrm{fm}^4$ with a resolution $a = 0.11\,\mathrm{fm}$ obtained from r_0. Different bare quark masses (am_q) were considered in the range $0.110, \ldots, 0.020, 0.002$. The smallest quark mass (corresponding to $\approx 3\,\mathrm{MeV}$) was certainly small enough to reach the ϵ-regime. Hybrid Monte Carlo with overlap fermions has problems when the topological charge changes. To avoid this an action was used which prevented topology change and the whole run stayed in the $Q = 0$ sector. The authors observed an overall good agreement with RMT. The fermion condensate, which is the only

JHEP11(2009)100

parameter to be fitted, was found to be $\Sigma(2\,\mathrm{GeV})^{1/3} = 0.251(7)(10)\mathrm{GeV}$ in the $\overline{\mathrm{MS}}$ scheme.

Our work is based on the parametrized fixed-point (FP) action which has been tested in detail in quenched QCD [24]. The exact FP Dirac operator satisfies the Ginsparg-Wilson relation

$$D^{\dagger}_{\mathrm{GW}} + D_{\mathrm{GW}} = D^{\dagger}_{\mathrm{GW}} 2R D_{\mathrm{GW}}\,, \tag{1}$$

where R is a local operator and is trivial in Dirac space. The parametrized FP action has many gauge paths and involves a special smearing with projection to the gauge group SU(3). As a consequence, hybrid Monte Carlo algorithms can not be used. In the work [25] we advised a partially global update with three nested accept/reject steps which can reach small quark masses even on coarse lattices. Several steps of this algorithm were developed in [26] using some earlier suggestions [27–30]. All the three steps are preconditioned. Pieces of the quark determinant are switched on gradually in the order of their computational expenses. The largest and most fluctuating part of the determinant is coming from the ultraviolet modes. We reduce these fluctuations by calculating the trace of $D^n_{\mathrm{FP}}, n = 1, \ldots, 4$ [26, 31, 32]. The ~ 100 lowest-lying modes are calculated and subtracted. The determinant of the reduced and subtracted D_{FP} is calculated stochastically [33–36]. For the determinant breakup we generalized the mass shifting method of [31]. For the strange quark we performed a root operation. Since the strange quark mass is not very small, we used a polynomial expansion to approximate this root operator. Recently we replaced the polynomial expansion by a rational approximation [37] which brought a $\approx 30\%$ performance gain in this part.

Due to the partial global updating procedure the algorithm, beyond a certain volume, scales with V^2 which constrains the size of lattices which can be considered. Due to the large number of subtracted low-lying modes, small quark mass is not a barrier.

We generated ~ 4000 equilibrated configurations in the Markov chain on an 12^4 lattice using the partially global algorithm discussed above. The distance between every second configurations in this chain is similar to that of two gauge configurations separated by a typical Metropolis gauge update sweep. We considered every tenth configurations from the Markov chain and performed the measurements on the remaining ~ 400 configurations. As will be described at the error-analysis of Σ later, on this set of configurations we estimated the autocorrelation time to be $\tau \approx 5$.

As it is well known, for a Dirac operator with good chiral properties it is difficult to tunnel between different topological sectors. In our simulation we observed only ~ 10 events of tunneling, which is certainly not enough to estimate the relative weights of the different sectors. However, this is also not needed for our purposes.

We fixed the lattice spacing from the Sommer parameter [38] $r_0 = 0.49\,\mathrm{fm}$ and found $a = 0.129(5)\,\mathrm{fm}$. Our box has the size $(1.6\,\mathrm{fm})^4$.

The Dirac operator D_{FP} has no exact chiral symmetry due to parametrization errors. As a consequence, the quark masses have an additive mass renormalization. The degenerate u, d and the s quark masses in the code are $M_{\mathrm{ud}} = 0.025$ and $M_{\mathrm{s}} = 0.103$. The additive renormalization was measured following the steps described in [39] and has the value $M_0 = 0.0147(3)$, as shown in figure 1. Subtracting the additive renormalization we

JHEP11(2009)100

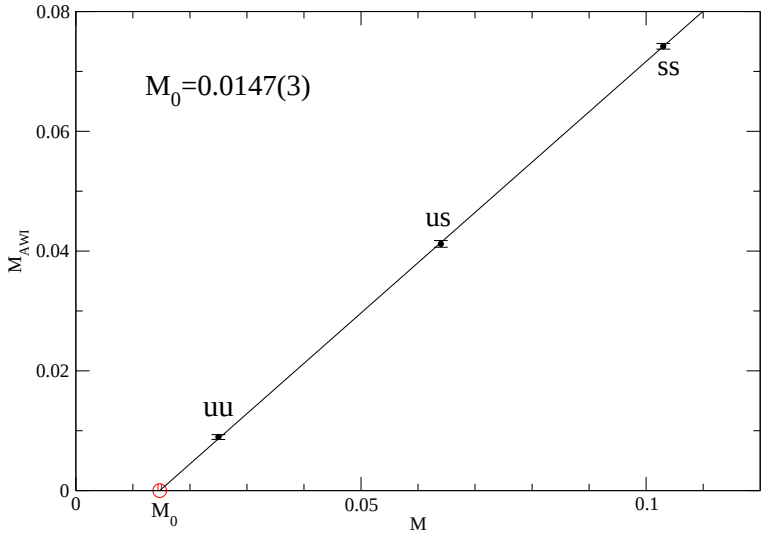

Figure 1. The axial Ward identity (AWI) mass for the three combinations of quark masses. The linear extrapolation to $M_{\rm AWI} = 0$ gives an additive mass renormalization $M_0 = 0.0147(3)$.

get the bare masses $m_{\rm ud} = 0.0103(3)$ and $m_{\rm s} = 0.0883(3)$ which corresponds to 16 MeV and 137 MeV, respectively.

As we mentioned above, a simulation with lighter quark masses would not be more expensive. In our case, however, a smaller $m_{\rm ud}$ were not useful either. RMT predicts the probability distribution $p_{\nu k}(\xi_{\nu k})$ for the k-th low-lying eigenvalue ($k = 1, 2, \dots$) of the Dirac operator in the topological sector ν. Denoting the corresponding eigenvalues of the (continuum) Dirac operator by $i\alpha_{\nu k}$, the variable $\xi_{\nu k}$ is related to the bare chiral condensate Σ as $\xi_{\nu k} = \alpha_{\nu k}\Sigma V$. Here V is the volume of the box. Figure 2 shows the prediction of RMT for the cumulative distributions $\int_0^{\xi_{\nu k}} d\xi p_{\nu k}(\xi)$ for $\nu = 0$ and $k = 1, 2, 3$. The distributions depend on $\mu_i = m_i \Sigma V$ where m_i are the quark masses. Decreasing the $m_{\rm ud}$ mass by more than a factor 10 (at fixed $m_{\rm s}$) the cumulative distributions practically remain unchanged. On the other hand sending the strange quark mass to infinity (at fixed $m_{\rm ud}$) we land on a $N_f = 2$ flavor theory with a visibly different distribution. The strange quark has a (modest) effect on our observables.

While the eigenvalues of the continuum Dirac operator lie on the imaginary axis the spectrum of lattice Dirac operators is more complicated. As it is well known, the spectrum of the Dirac operator satisfying the Ginsparg-Wilson relation with $2R = 1$ lies on the circle $|\lambda - 1| = 1$. In our case where $2R$ is different from 1, it is convenient to introduce the rescaled operator $\hat{D}_{\rm GW} = \sqrt{2R} D_{\rm GW} \sqrt{2R}$, for which the $2R$ factor is eliminated in the GW relation, and the spectrum lies on the circle. (In fact, our operator $2R$ for the low-lying modes is effectively a constant close to 1 within a few percent.) To relate the eigenvalues on the GW circle to those appearing in the RMT (or in general, in continuum expressions) it is natural to use the stereographic projection

$$i\alpha = \frac{\lambda}{1 - \lambda/2}\,. \tag{2}$$

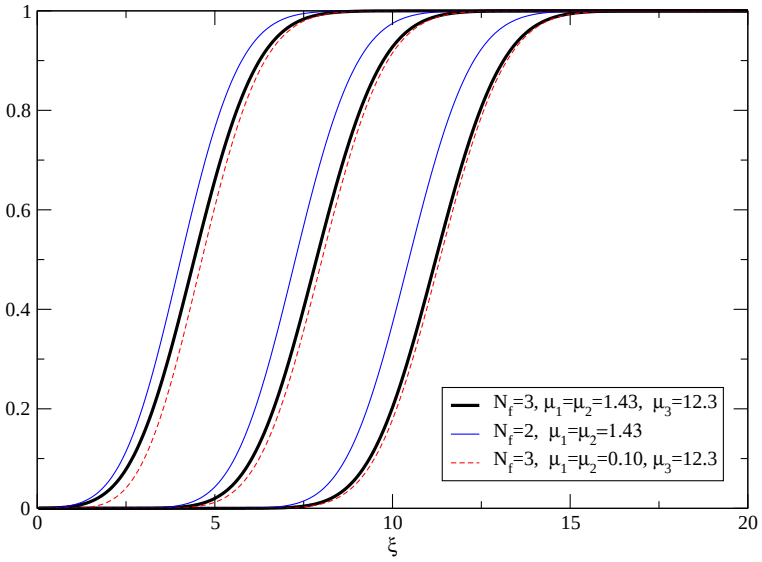

Figure 2. Random Matrix Theory prediction for the cumulative distribution of $\xi = \xi_{\nu k} = \alpha_{\nu k}\Sigma V$, where $i\alpha_{\nu k}$ is the k-th eigenvalue of the continuum Dirac operator in a gauge background with topological charge ν, and $\mu_i = m_i \Sigma V$. Here the $\nu = 0$ results are shown, but the picture is similar for $\nu = 1, 2$.

(Note that the non-local operator $\hat{D}_{\rm GW}/\left(1 - \frac{1}{2}\hat{D}_{\rm GW}\right)$ anticommutes with γ_5.)

As figure 3 shows, the low-lying eigenvalues of $D_{\rm FP}(m)$ (which we obtain during our simulation) are close but not exactly on the GW circle, hence we project them first horizontally onto the GW circle, and make the stereographic projection in the next step. This is justified by the observation that making a systematic GW improvement of $D_{\rm FP}$ towards $D_{\rm GW}$ the imaginary part of the eigenvalues stays practically constant – they move horizontally to the GW circle. The values of α obtained by this procedure are then compared with the RMT predictions.

Having the probability distributions from RMT we can calculate the ratios $\langle \xi_{\nu k} \rangle / \langle \xi_{\nu' k'} \rangle$, where the factor ΣV cancels. These predictions are compared with the measured ratios in figure 4, where all the ratios in the topological sectors $\nu = 1, 2, 3$ for the first three lowest eigenvalues are shown.

At this point we have to discuss the way we identify the topological sectors. According to the index theorem [40] one can identify the topological charge from the zero modes of a Ginsparg-Wilson Dirac operator. However, our $D_{\rm FP}$ has no exact chiral symmetry and has modes on the real axis. Occasionally, the real eigenvalue λ might be even far from zero in which case the topological interpretation is uncertain. We note here that using an exact Ginsparg-Wilson operator (with kernel $D_{\rm FP}$) for measuring the topological charge is not a good solution to this problem. The overlap just projects most of the real eigenvalues to the point $\lambda = 0$.

Following the intuitive picture that topology is related to extended objects we investigated for real eigenvalues the correlation between the eigenvalue and the inverse

JHEP11(2009)100

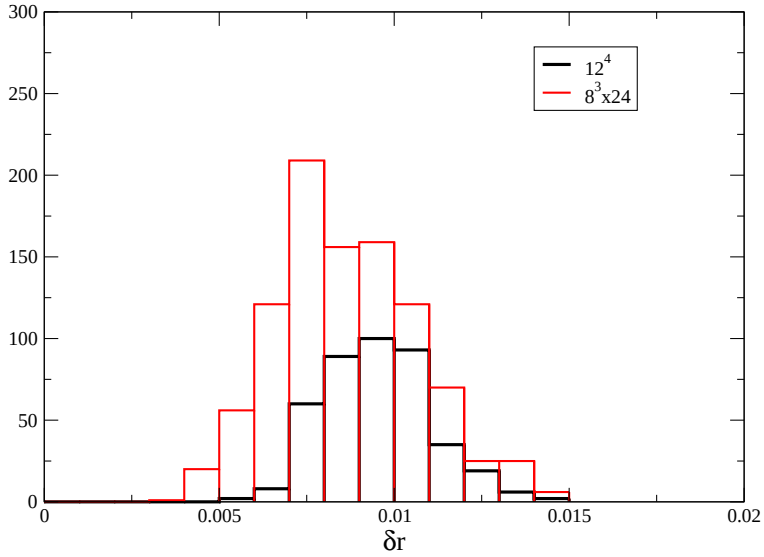

Figure 3. The histogram of the deviation from the circle, $\delta r = 1 - |\lambda - 1|$, for the eigenvalues of $D_{\rm FP}$ on $8^3 \times 24$ and 12^4 lattices for the complex eigenvalues with $|{\rm Im}\lambda| < 0.1$, using the present mass parameters.

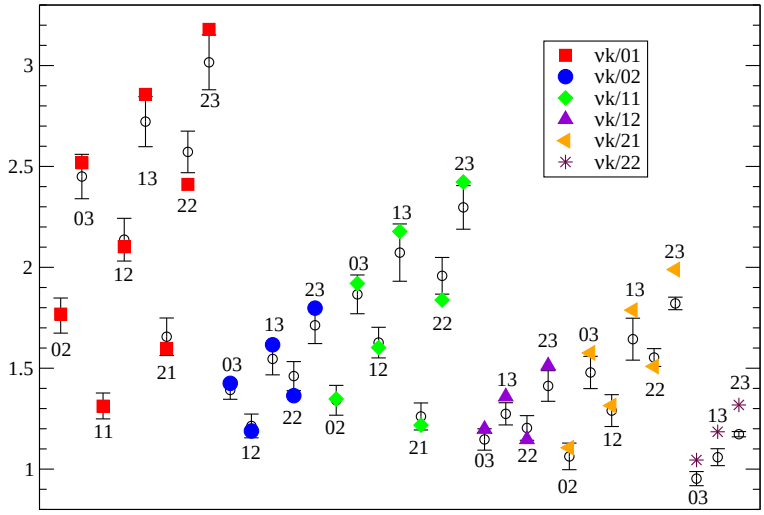

Figure 4. Ratios of expectation values $\langle \alpha_{\nu k} \rangle$ obtained from simulations compared to the results of RMT, where νk is indexing the k-th lowest eigenvalue in the topological sector ν. The different symbols refer to the denominator while νk of the numerator is indicated at the data points. For example, the highest ratio with value ≈ 3 in the figure refers to $\langle \xi_{23} \rangle / \langle \xi_{01} \rangle$

.

participation ratio (IPR) of the corresponding eigenvector. Here IPR is given by $\sum_x (\sum_{i=1}^{12} |\psi_i^{(\lambda)}(x)|^2)^2$ for a normalized eigenvector $\psi^{(\lambda)}$, and it is inversely proportional to the size of the effective support of the eigenfunction. As figure 5 shows, there is a strong correlation indeed. As λ is moving away from zero, the IPR increases indicating

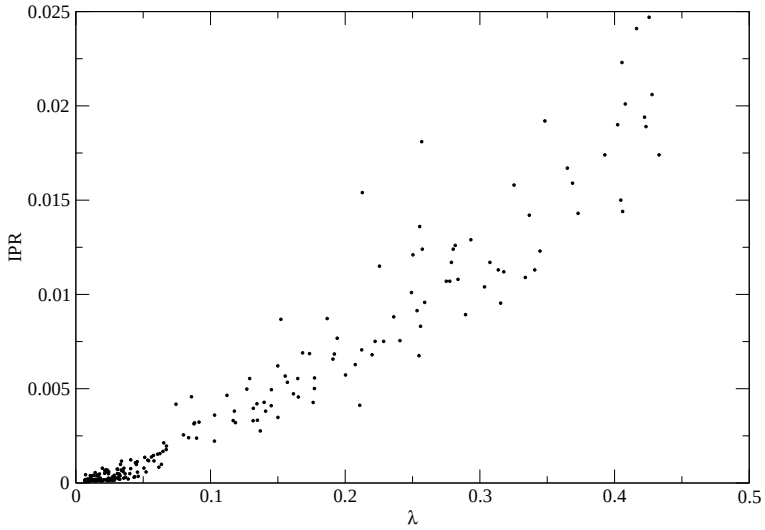

Figure 5. The inverse participation ratio $\sum_x (\sum_{i=1}^{12} |\psi_i^{(\lambda)}(x)|^2)^2$ for *real* eigenvalues $\lambda(D_{\rm FP})$ vs. the eigenvalue. Eigenvectors with larger real λ have smaller extension in agreement with the expectations.

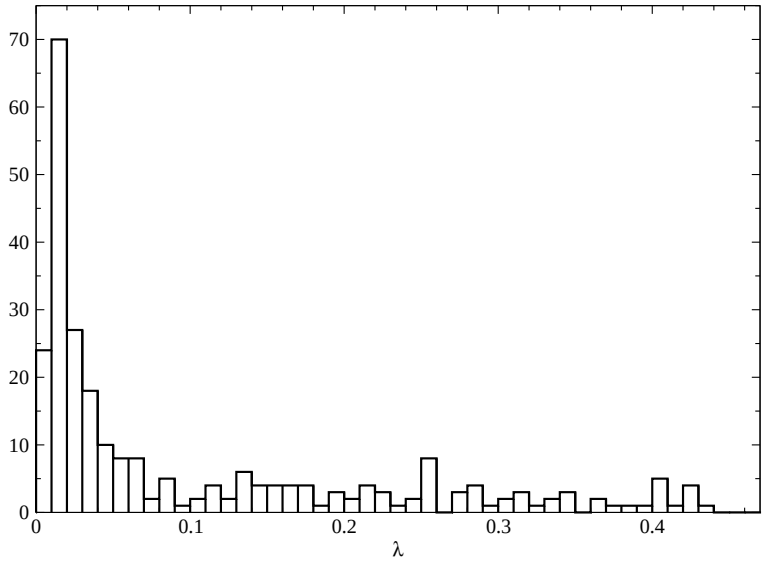

Figure 6. Histogram of $\lambda(D_{\rm FP})$ for the real eigenvalues. Note that there are 231 configurations with no real eigenvalues which, of course, do not enter this plot.

that the wave function becomes more and more localized. Figure 6 demonstrates that the real eigenvalues $\lambda(D_{\rm FP})$ are strongly concentrated in a small region close to zero. The histogram of $\lambda(D_{\rm FP})$ has a large, narrow peak followed by a long tail.

We shall use the small real eigenvalues and the chirality of the corresponding eigenvectors to assign a topological charge to a given configuration. Obviously, this involves some freedom of choice.

It turns out, however, that the ambiguity of assigning the topological charge based on

JHEP11(2009)100

the smallest real eigenvalues of $D_{\rm FP}$ in our case does not affect significantly the estimated value of the condensate. During the update procedure we have on each configuration the eigenvalues and eigenvectors for the smallest 96 values of $|\lambda|$. Out of 414 configurations we analyzed, 231 configurations have no real eigenvalue at all. (This reflects the good chiral properties of $D_{\rm FP}$.) For these configurations the assignment to $\nu = 0$ is unambiguous. Further, one can assign to the $\nu = 0$ sector those configurations which have no real eigenvalues below some cut c_1. That means that we consider eigenvalues with $\lambda > c_1$ as (localized) lattice artifacts. Taking $c_1 = 0.1$, 0.08, 0.06, 0.04 we obtained 284, 288, 296, 313 configurations, respectively. This choice influences the fit value of $a\Sigma^{1/3}$ by $\sim 0.3\%$, less than the statistical error of $\sim 1\%$. The value of the condensate was determined from the $\nu = 0$ sector in two different ways, from the distribution of the $k = 1$ eigenvalues alone and from the $k = 2, 3$ eigenvalues. The results were consistent, practically with the same statistical error.

The results for $\nu \geq 1$ were used only to check the consistency to the RMT predictions. To assign the topological charge in this case we introduced two cuts, $c_0 \leq c_1$. To decrease the ambiguity of the assignment, the configuration was discarded if it had a real eigenvalue in the interval $[c_0, c_1]$. Then the total chirality of the modes with $\lambda < c_0$ was used as the topological charge. We have chosen $c_0 = 0.03$ and $c_1 = 0.1$ in the plots for $\nu = 1, 2$ described later, but any other reasonable choice leads to very similar picture.

Figure 8 compares the cumulative distributions of the first three eigenvalues in the $\nu = 0$ topological sector obtained using the overlap improved fixed-point Dirac operator $D_{\rm GW}$ vs. $D_{\rm FP}$ in the measurement. The distributions are very similar showing that the two operators are close to each other. The $k = 1$ distribution from $D_{\rm GW}$ has a tail at small eigenvalues (i.e. has a smaller gap than $D_{\rm FP}$) demonstrating a systematic error one obtains when using different Dirac operators for the generation of the configurations and for the measurements: the small eigenvalues are less efficiently suppressed.

In figure 9 the cumulative distributions of the $D_{\rm FP}$ operator are compared with RMT for the $\nu = 0$ topological sector. The only matching parameter is the bare condensate Σ which enters the RMT predictions through $\mu_i = m_i \Sigma V$ and in $\alpha \Sigma V$. Using the value $a = 0.129(5)\,\mathrm{fm}$ for our lattice spacing we obtained the result for this bare quantity $\Sigma^{1/3} = 0.291(4)(10)\,\mathrm{GeV}$. Both errors are statistical. The first error comes from the statistical errors of the measured distributions, the second one is due to the error in the lattice scale a.

For the determination of the statistical error of $a\Sigma^{1/3}$ we used the jack-knife method with different length of the bins, between 5 and 20. This gave a rough estimate for the autocorrelation time $\tau \approx 5$ (assuming an auto-correlation with a single exponential). We took this into account in estimating the statistical error.

Comparing the shape of distributions in figure 9 one sees that although the mean values of the distributions agree well with the RMT prediction, the observed distribution of the first eigenvalue is narrower than the theoretical prediction, while the shapes of the $k = 2$ and $k = 3$ distributions agree well. This might be a consequence of our relatively small volume, $L \approx 1.6\,\mathrm{fm}$. One expects that this affects more the distribution of the $k = 1$ eigenvalue, especially at small λ values, which correspond to more extended wave functions. On the contrary, discretization errors should affect more the largest eigenvalues which correspond to shorter wave length. However, our FP Dirac operator is expected to

JHEP11(2009)100

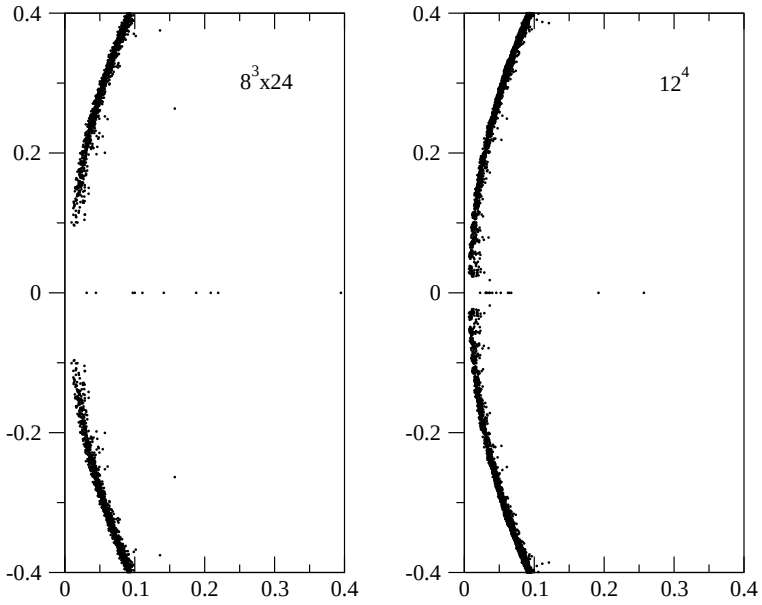

Figure 7. The spectrum of $D_{\rm FP}$ for 50 configurations on $8^3 \times 24$ and 12^4 lattices, at the same bare mass parameters and gauge coupling.

have small discretization errors even at such coarse lattices.

In figures 10), (11 the rescaled cumulative distributions for $\nu = 1$ and $\nu = 2$ cases (using the same value of Σ by rescaling) are compared with the RMT predictions.

The result above receives a small correction due to the fact that, for simplifying the presentation, we suppressed a technical complication. As mentioned before the exact fixed-point operator satisfies a Ginsparg-Wilson relation with a local operator $2R$. For this reason the quark mass enters in a simple additive way in the form $\hat{D} + m(1 - \hat{D}/2)$, where $\hat{D} = \sqrt{2R} D_{\rm FP} \sqrt{2R}$. Effectively the operator $2R$ behaves in the infrared like a constant close to 1. Its expectation value for the lowest ~ 100 eigenvectors is 1.05 within 1%. Using the spectrum of $\hat{D}$ (which is in fact identical to that of $2RD_{\rm FP}$) the matching with RMT gives the slightly changed result $\Sigma^{1/3} = 0.286(4)(10)\,\mathrm{GeV}$.

In the language of a ferromagnetic O(N) model one should interpret Σ as the *absolute value* of the magnetization in the finite volume V. This differs from the value Σ_∞ defined in the infinite volume by a finite-size correction which can be calculated in ChPT. In the presence of the magnetic field h the orientation of magnetization is controlled by the Boltzmann factor $\exp(hM\cos\theta)$ where M is the total magnetization. This gives

$$\langle M_\parallel \rangle = M \frac{Y_N'(hM)}{Y_N(hM)}\,, \tag{3}$$

where $Y_N(z)$ is related to the modified Bessel functions. Comparing this expression with the result of ChPT [7] we get for $N = 4$ (corresponding to two flavors) $\Sigma = \rho\Sigma_\infty$, where

$$\rho = \left(1 + \frac{3}{2}\frac{\beta_1}{F^2 L^2}\right)\,. \tag{4}$$

JHEP11(2009)100

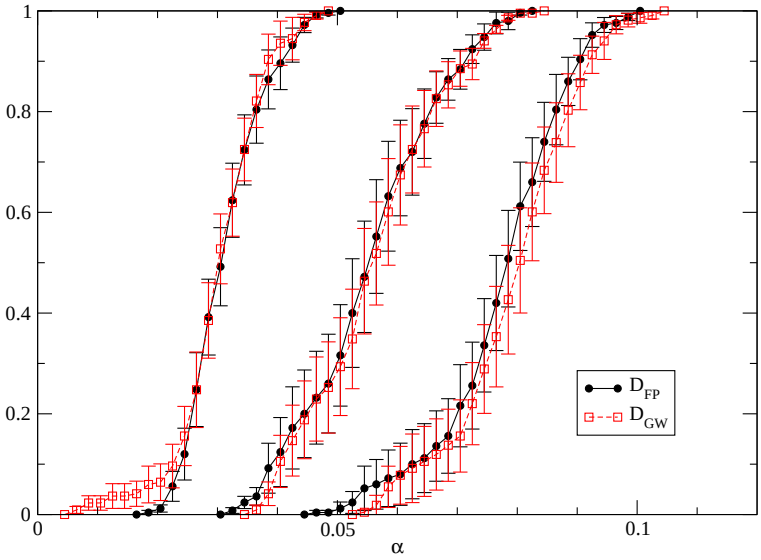

Figure 8. The cumulative distributions in the $\nu = 0$ topological sector for the three lowest complex eigenvalues as measured with $D_{\rm FP}$ and with the overlap operator $D_{\rm GW}$ using the fixed-point operator as kernel.

Here the shape coefficient β_1 takes the value 0.14046 for a symmetric box [7]. The one-loop finite-size correction to the order parameter (magnetization in the example above) has been calculated for the $\mathrm{SU}(N_f) \times \mathrm{SU}(N_f)$ symmetry group in [5, 6], for the $\mathrm{O}(N)$ group in [41] and up to the two-loop level in [7].

Neglecting the strange quark contribution in the finite size effects we use the two-flavor result to correct the measured bare $\Sigma^{1/3} = 0.286(4)(10)\,\mathrm{GeV}$ by the one-loop finite size correction to obtain $\Sigma^{1/3}_{\infty} = \Sigma^{1/3}/1.119 = 0.255(4)(10)\,\mathrm{GeV}$.

To relate this bare quantity to the generally used $\overline{\rm MS}$ scheme one still needs the corresponding renormalization factor. This has been calculated in [42]. The main points of this calculation are summarized in the appendix. With the conversion factor 0.82(3) we obtain

$$[\Sigma_{\overline{\rm MS}}(2\,\mathrm{GeV})]^{1/3} = 0.239(12)\,\mathrm{GeV}\,. \tag{5}$$

Acknowledgments

We thank Gilberto Colangelo, Stephan Dürr, Jürg Gasser, Anna Hasenfratz and the members of the BGR Collaboration for valuable discussions. We also thank the LRZ in Munich and CSCS in Manno for support. The analysis was done on the PC clusters of ITP in Bern. The authors acknowledge support by DFG project SFB/TR-55. The "Albert Einstein Center for Fundamental Physics" at Bern University is supported by the "Innovations-und Kooperationsprojekt C-13" of the Schweizerischer Nationalfonds.

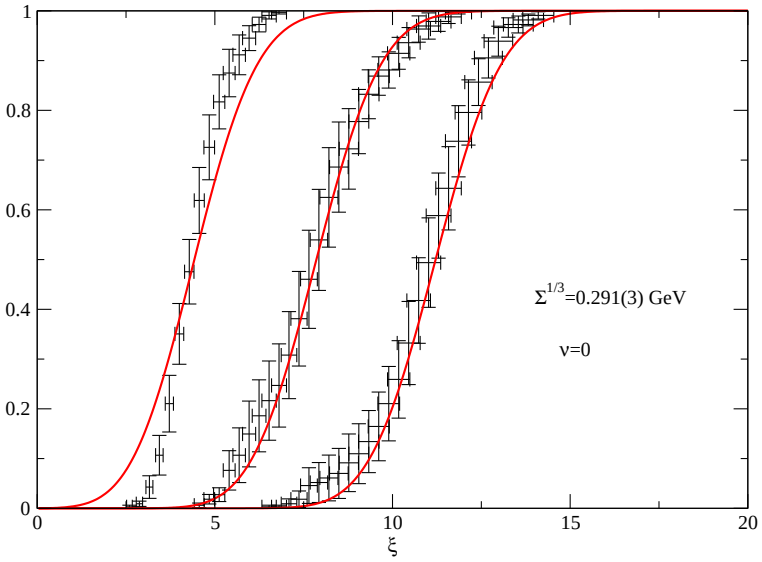

Figure 9. The cumulative distribution of $\xi_{\nu k} = \alpha_{\nu k}\Sigma V$ for $\nu = 0$, $k = 1, 2, 3$. Here α is obtained from $\lambda(D_{\rm FP})$ by stereographic projection described in the text, and is rescaled using $\Sigma^{1/3} = 0.291(4)\,\text{GeV}$. The continuous line is the RMT prediction at $\mu_1 = \mu_2 = m_{\rm ud}\Sigma V = 1.43$ and $\mu_3 = m_{\rm s}\Sigma V = 12.3$.

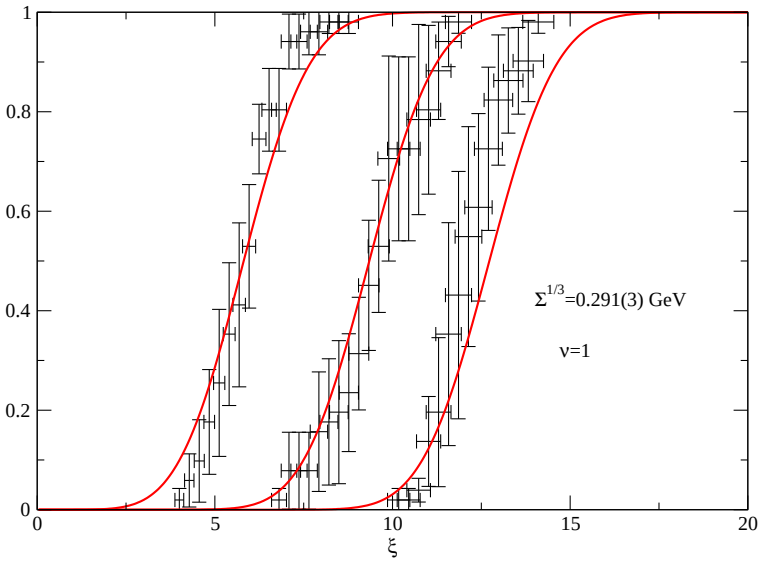

Figure 10. The cumulative distribution of $\xi_{\nu k} = \alpha_{\nu k}\Sigma V$ for $\nu = 1$, $k = 1, 2, 3$.

A. Renormalization of the condensate in the $\overline{MS}$ scheme

The bare lattice scalar density is not universal, it depends on the lattice action and it needs renormalization. The conventional way is to express the result in $\overline{\rm MS}$ scheme at some given scale, e.g. $\mu_0 = 2\,\text{GeV}$.

JHEP11(2009)100

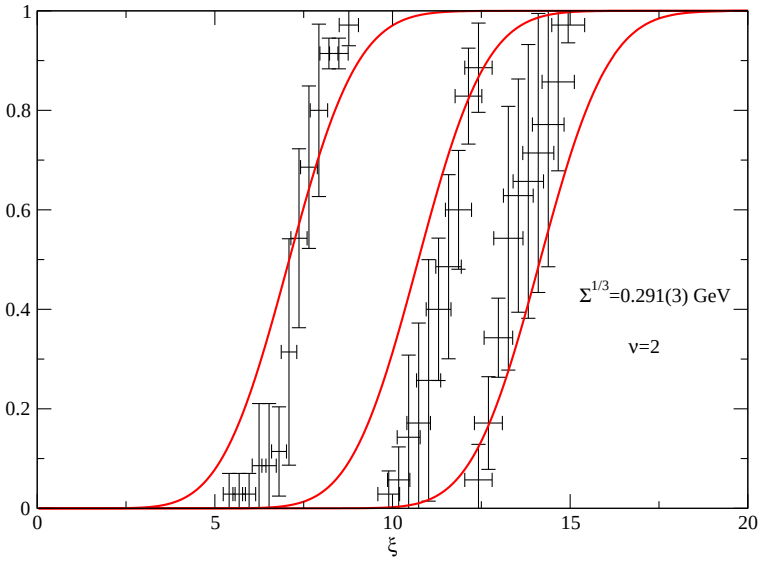

Figure 11. The cumulative distribution of $\xi_{\nu k} = \alpha_{\nu k}\Sigma V$ for $\nu = 2$, $k = 1, 2, 3$.

To relate the bare lattice result to $\overline{\text{MS}}$ scheme one generally uses the Rome-Southhampton RI/MOM method [43]. In this method one introduces an intermediate scheme RI (or RI′[1]) where some Green's functions of the actual operator (calculated in a fixed gauge) are equated to their corresponding Born terms at a given scale $p^2 = \mu^2$.

In the first step one relates the bare lattice operator non-perturbatively to its renormalized counterpart in the RI scheme

$$\mathcal{O}_{\text{R}}^{\text{RI}}(\mu) = Z_{\mathcal{O}}^{\text{RI,lat}}(\mu, a)\mathcal{O}_{\text{bare}}^{\text{lat}}(a)\,. \tag{A.1}$$

The matching scale μ is restricted by two conditions: It should be sufficiently large to avoid non-perturbative effects and small enough to avoid large cut-off effects. For the scalar density, the non-perturbative matching was done in [42], using a technique which removes a large part of $\text{O}(a)$ cut-off effects.

In the second step one relates the renormalized operators in the RI and $\overline{\text{MS}}$ schemes in perturbation theory

$$\mathcal{O}_{\text{R}}^{\overline{\text{MS}}}(\mu) = Z^{\overline{\text{MS}},\text{RI}}(\mu)\mathcal{O}_{\text{R}}^{\text{RI}}(\mu)\,. \tag{A.2}$$

Obviously, the value of μ must lie in the perturbative regime. The factor $Z^{\overline{\text{MS}},\text{RI}}(\mu)$ has been calculated up to NNLO [44] and NNNLO [45]. Combining (A.1) and (A.2), we obtain the matching factor connecting the bare lattice and the renormalized $\overline{\text{MS}}$ results

$$\mathcal{Z}_{\mathcal{O}}^{\overline{\text{MS}},\text{lat}}(\mu, a) = Z^{\overline{\text{MS}},\text{RI}}(\mu)Z_{\mathcal{O}}^{\text{RI,lat}}(\mu, a)\,. \tag{A.3}$$

As the expansion parameter in the perturbative series is the running coupling $\alpha(\mu)$ of QCD, we need to determine it for the scale μ where the matching is done. The running of

[1]These schemes differ in their definition of the quark field renormalization factor Z_q.

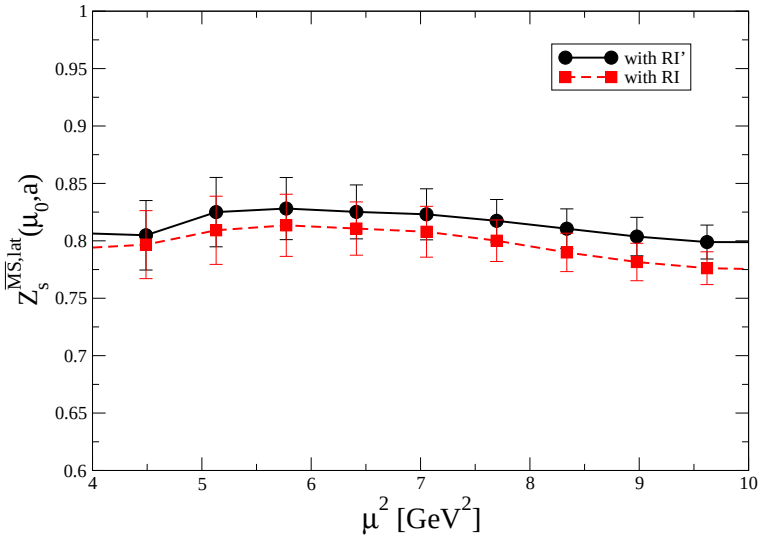

Figure 12. The renormalization factor $\mathcal{Z}_{\rm s}^{\overline{\rm MS},\rm lat}(\mu_0, a)$ for the scalar density, connecting the $\overline{\rm MS}$ and lattice schemes, at $\mu_0 = 2\,\text{GeV}$, obtained using RI and RI′ schemes at the intermediate step vs. the matching scale μ.

α is described by the differential equation

$$\frac{d\alpha(\mu)}{d\ln\mu^2} = \beta(\alpha)\,, \tag{A.4}$$

where the 4-loop β-function in $\overline{\rm MS}$ scheme is given in [46]. As initial condition we use $\alpha(2\,\text{GeV}) = 0.2904$ from [47].[2] The procedure described above is carried out at several matching scales $\mu \geq 2\,\text{GeV}$.

In the third step Renormalization Group technique is used to obtain the desired conversion factor $\mathcal{Z}_{\rm s}^{\overline{\rm MS},\rm lat}(\mu_0, a)$ for the scalar density at $\mu_0 = 2\,\text{GeV}$,

$$\mathcal{Z}_{\rm s}^{\overline{\rm MS},\rm lat}(\mu_0, a) = \mathcal{Z}_{\rm s}^{\overline{\rm MS},\rm lat}(\mu, a)\exp\left(-\int_{\alpha(\mu_0)}^{\alpha(\mu)} d\alpha\frac{\gamma_s(\alpha)}{\beta(\alpha)}\right)\,. \tag{A.5}$$

Here, due to the relation $Z_s = Z_m^{-1}$, the anomalous dimension γ_s is related to the mass anomalous dimension by $\gamma_{\rm s} = -\gamma_{\rm m}$. The latter has been calculated to four loops in [49, 50].

In figure 12, we plot our result $\mathcal{Z}_{\rm s}^{\overline{\rm MS},\rm lat}(\mu_0, a)$ at $\mu_0 = 2\,\text{GeV}$ vs. the matching scale μ for the intermediate schemes RI and RI′. If the non-perturbative, cut-off and higher order perturbative effects were negligible, the two curves would coincide and would be independent of the choice of μ. Taking the average values for $2\,\text{GeV} \leq \mu \leq 3\,\text{GeV}$ and taking into account the slight difference between the curves, we get

$$\mathcal{Z}_{\rm s}^{\overline{\rm MS},\rm lat}(\mu_0 = 2\,\text{GeV}, a) = 0.82(3) \tag{A.6}$$

[2]This result is obtained by using the PDG value $\alpha(\rm M_Z) = 0.1176 \pm 0.002$ [48] and running it from 5-flavors down to 3-flavors, across the $\rm m_b$ and $\rm m_c$ thresholds

JHEP11(2009)100

References

[1] S. Weinberg, *Phenomenological Lagrangians*, *Physica* **A 96** (1979) 327 [SPIRES].

[2] J. Gasser and H. Leutwyler, *On the low-energy structure of QCD*, *Phys. Lett.* **B 125** (1983) 321 [SPIRES]; *Low-energy theorems as precision tests of QCD*, *Phys. Lett.* **B 125** (1983) 325 [SPIRES].

[3] J. Gasser and H. Leutwyler, *Chiral perturbation theory to one loop*, *Annals Phys.* **158** (1984) 142.

[4] J. Gasser and H. Leutwyler, *Chiral perturbation theory: expansions in the mass of the strange quark*, *Nucl. Phys.* **B 250** (1985) 465 [SPIRES].

[5] J. Gasser and H. Leutwyler, *Light quarks at low temperatures*, *Phys. Lett.* **B 184** (1987) 83 [SPIRES]; *Thermodynamics of chiral symmetry*, *Phys. Lett.* **B 188** (1987) 477 [SPIRES].

[6] J. Gasser and H. Leutwyler, *Spontaneously broken symmetries: effective Lagrangians at finite volume*, *Nucl. Phys.* **B 307** (1988) 763 [SPIRES].

[7] P. Hasenfratz and H. Leutwyler, *Goldstone boson related finite size effects in field theory and critical phenomena with O(N) symmetry*, *Nucl. Phys.* **B 343** (1990) 241 [SPIRES].

[8] F.C. Hansen, *Finite size effects in spontaneously broken* $\mathrm{SU}(N) \times \mathrm{SU}(N)$ *theories*, *Nucl. Phys.* **B 345** (1990) 685 [SPIRES].

[9] E.V. Shuryak and J.J.M. Verbaarschot, *Random matrix theory and spectral sum rules for the Dirac operator in QCD*, *Nucl. Phys.* **A 560** (1993) 306 [hep-th/9212088] [SPIRES]; J.J.M. Verbaarschot and T. Wettig, *Random matrix theory and chiral symmetry in QCD*, *Ann. Rev. Nucl. Part. Sci.* **50** (2000) 343 [hep-ph/0003017] [SPIRES]; P.H. Damgaard and S.M. Nishigaki, *Distribution of the* k^{th} *smallest Dirac operator eigenvalue*, *Phys. Rev.* **D 63** (2001) 045012 [hep-th/0006111] [SPIRES].

[10] R.G. Edwards, U.M. Heller, J.E. Kiskis and R. Narayanan, *Quark spectra, topology and random matrix theory*, *Phys. Rev. Lett.* **82** (1999) 4188 [hep-th/9902117] [SPIRES].

[11] W. Bietenholz, K. Jansen and S. Shcheredin, *Spectral properties of the overlap Dirac operator in QCD*, *JHEP* **07** (2003) 033 [hep-lat/0306022] [SPIRES].

[12] W. Bietenholz, T. Chiarappa, K. Jansen, K.I. Nagai and S. Shcheredin, *Axial correlation functions in the* ϵ*-regime: A numerical study with overlap fermions*, *JHEP* **02** (2004) 023 [hep-lat/0311012] [SPIRES].

[13] L. Giusti, M. Lüscher, P. Weisz and H. Wittig, *Lattice QCD in the* ϵ*-regime and random matrix theory*, *JHEP* **11** (2003) 023 [hep-lat/0309189] [SPIRES].

[14] L. Giusti, P. Hernández, M. Laine, P. Weisz and H. Wittig, *Low-energy couplings of QCD from current correlators near the chiral limit*, *JHEP* **04** (2004) 013 [hep-lat/0402002] [SPIRES].

[15] R.G. Edwards, *Topology and low lying fermion modes*, *Nucl. Phys. (Proc. Suppl.)* **106** (2002) 38 [hep-lat/0111009] [SPIRES].

[16] T.A. DeGrand and S. Schaefer, *Improving meson two-point functions in lattice QCD*, *Comput. Phys. Commun.* **159** (2004) 185 [hep-lat/0401011] [SPIRES].

[17] L. Giusti, C. Hölbling, M. Lüscher and H. Wittig, *Numerical techniques for lattice QCD in the* ϵ*-regime*, *Comput. Phys. Commun.* **153** (2003) 31 [hep-lat/0212012] [SPIRES].

[18] L. Giusti and S. Necco, *Spontaneous chiral symmetry breaking in QCD: a finite-size scaling study on the lattice*, *JHEP* **04** (2007) 090 [hep-lat/0702013] [SPIRES].

JHEP11(2009)100

[19] P.H. Damgaard, *Quenched and unquenched chiral perturbation theory in the ϵ-regime*, *Nucl. Phys. (Proc. Suppl.)* **128** (2004) 47 [hep-lat/0310037] [SPIRES].

[20] H. Neuberger, *Exactly massless quarks on the lattice*, *Phys. Lett.* **B 417** (1998) 141 [hep-lat/9707022] [SPIRES]; *More about exactly massless quarks on the lattice*, *Phys. Lett.* **B 427** (1998) 353 [hep-lat/9801031] [SPIRES].

[21] T.A. DeGrand and S. Schaefer, *Physics issues in simulations with dynamical overlap fermions*, *Phys. Rev.* **D 71** (2005) 034507 [hep-lat/0412005] [SPIRES]; *Chiral properties of two-flavor QCD in small volume and at large lattice spacing*, *Phys. Rev.* **D 72** (2005) 054503 [hep-lat/0506021] [SPIRES]; *Dynamical overlap fermions: techniques and results. Simulations and physics results*, PoS(LAT2005)140 [hep-lat/0508025] [SPIRES].

[22] T. DeGrand, Z. Liu and S. Schaefer, *Quark condensate in two-flavor QCD*, *Phys. Rev.* **D 74** (2006) 094504 [*Erratum ibid.* **D 74** (2006) 099904] [hep-lat/0608019] [SPIRES].

[23] JLQCD collaboration, H. Fukaya et al., *Two-flavor lattice QCD simulation in the ϵ-regime with exact chiral symmetry*, *Phys. Rev. Lett.* **98** (2007) 172001 [hep-lat/0702003] [SPIRES].

[24] P. Hasenfratz et al., *The construction of generalized Dirac operators on the lattice*, *Int. J. Mod. Phys.* **C 12** (2001) 691 [hep-lat/0003013] [SPIRES];
P. Hasenfratz, S. Hauswirth, T. Jorg, F. Niedermayer and K. Holland, *Testing the fixed-point QCD action and the construction of chiral currents*, *Nucl. Phys.* **B 643** (2002) 280 [hep-lat/0205010] [SPIRES];
BGR collaboration, C. Gattringer et al., *Quenched spectroscopy with fixed-point and chirally improved fermions*, *Nucl. Phys.* **B 677** (2004) 3 [hep-lat/0307013] [SPIRES];
Bern-Graz-Regensburg collaboration, P. Hasenfratz, K.J. Juge and F. Niedermayer, *New results on cut-off effects in spectroscopy with the fixed point action*, *JHEP* **12** (2004) 030 [hep-lat/0411034] [SPIRES].

[25] A. Hasenfratz, P. Hasenfratz and F. Niedermayer, *Simulating full QCD with the fixed point action*, *Phys. Rev.* **D 72** (2005) 114508 [hep-lat/0506024] [SPIRES].

[26] A. Hasenfratz and F. Knechtli, *Simulation of dynamical fermions with smeared links*, *Comput. Phys. Commun.* **148** (2002) 81 [hep-lat/0203010] [SPIRES].

[27] A. Hasenfratz and F. Knechtli, *Simulation of dynamical fermions with smeared links*, *Comput. Phys. Commun.* **148** (2002) 81 [hep-lat/0203010] [SPIRES].

[28] M. Creutz, *Algorithms for simulating fermions*, in *Quantum fields on the computer*, World Scientific Publishing, Singapore (1992).

[29] A. Hasenfratz and A. Alexandru, *Evaluating the fermionic determinant of dynamical configurations*, *Phys. Rev.* **D 65** (2002) 114506 [hep-lat/0203026] [SPIRES]; *Partial-global stochastic Metropolis update for dynamical smeared link fermions*, *Phys. Rev.* **D 66** (2002) 094502 [hep-lat/0207014] [SPIRES].

[30] Alpha collaboration, F. Knechtli and U. Wolff, *Dynamical fermions as a global correction*, *Nucl. Phys.* **B 663** (2003) 3 [hep-lat/0303001] [SPIRES].

[31] M. Hasenbusch, *Speeding up the Hybrid-Monte-Carlo algorithm for dynamical fermions*, *Phys. Lett.* **B 519** (2001) 177 [hep-lat/0107019] [SPIRES].

[32] P. de Forcrand, *UV-filtered fermionic Monte Carlo*, *Nucl. Phys. (Proc. Suppl.)* **73** (1999) 822 [hep-lat/9809145] [SPIRES].

JHEP11(2009)100

[33] A.D. Kennedy and J. Kuti, *Noise without noise: a new Monte Carlo method*, *Phys. Rev. Lett.* **54** (1985) 2473 [SPIRES].

[34] A.D. Kennedy, J. Kuti, S. Meyer and B.J. Pendleton, *Quarks, noise, and the lattice*, *Phys. Rev.* **D 38** (1988) 627 [SPIRES].

[35] B. Joo, I. Horvath and K.F. Liu, *The Kentucky noisy Monte Carlo algorithm for Wilson dynamical fermions*, *Phys. Rev.* **D 67** (2003) 074505 [hep-lat/0112033] [SPIRES].

[36] I. Montvay and E. Scholz, *Updating algorithms with multi-step stochastic correction*, *Phys. Lett.* **B 623** (2005) 73 [hep-lat/0506006] [SPIRES].

[37] M. Weingart, *Stochastic estimator of the s quark determinant in full QCD simulation*, Diploma work, University of Bern, Bern Switzerland (2007).

[38] R. Sommer, *A new way to set the energy scale in lattice gauge theories and its applications to the static force and α_s in* SU(2) *Yang-Mills theory*, *Nucl. Phys.* **B 411** (1994) 839 [hep-lat/9310022] [SPIRES].

[39] A. Hasenfratz, P. Hasenfratz, F. Niedermayer, D. Hierl and A. Schäfer, *First results in QCD with $2+1$ light flavors using the fixed-point action*, PoS(LAT2006)178 [hep-lat/0610096] [SPIRES].

[40] P. Hasenfratz, V. Laliena and F. Niedermayer, *The index theorem in QCD with a finite cut-off*, *Phys. Lett.* **B 427** (1998) 125 [hep-lat/9801021] [SPIRES].

[41] H. Neuberger, *A better way to measure f_π in the linear sigma model*, *Phys. Rev. Lett.* **60** (1988) 889 [SPIRES]; *Soft pions in large boxes*, *Nucl. Phys.* **B 300** (1988) 180 [SPIRES].

[42] V. Maillart and F. Niedermayer, *A specific lattice artefact in non-perturbative renormalization of operators*, arXiv:0807.0030 [SPIRES].

[43] G. Martinelli, C. Pittori, C.T. Sachrajda, M. Testa and A. Vladikas, *A general method for nonperturbative renormalization of lattice operators*, *Nucl. Phys.* **B 445** (1995) 81 [hep-lat/9411010] [SPIRES].

[44] E. Franco and V. Lubicz, *Quark mass renormalization in the MS-bar and RI schemes up to the NNLO order*, *Nucl. Phys.* **B 531** (1998) 641 [hep-ph/9803491] [SPIRES].

[45] K.G. Chetyrkin and A. Retey, *Renormalization and running of quark mass and field in the regularization invariant and MS-bar schemes at three and four loops*, *Nucl. Phys.* **B 583** (2000) 3 [hep-ph/9910332] [SPIRES].

[46] T. van Ritbergen, J.A.M. Vermaseren and S.A. Larin, *The four-loop β-function in quantum chromodynamics*, *Phys. Lett.* **B 400** (1997) 379 [hep-ph/9701390] [SPIRES].

[47] Y. Aoki et al., *Non-perturbative renormalization of quark bilinear operators and B_K using domain wall fermions*, *Phys. Rev.* **D 78** (2008) 054510 [arXiv:0712.1061] [SPIRES].

[48] Particle Data Group collaboration, W.M. Yao et al., *Review of particle physics*, *J. Phys.* **G 33** (2006) 1 [SPIRES].

[49] K.G. Chetyrkin, *Quark mass anomalous dimension to $O(\alpha_s^4)$*, *Phys. Lett.* **B 404** (1997) 161 [hep-ph/9703278] [SPIRES].

[50] J.A.M. Vermaseren, S.A. Larin and T. van Ritbergen, *The 4-loop quark mass anomalous dimension and the invariant quark mass*, *Phys. Lett.* **B 405** (1997) 327 [hep-ph/9703284] [SPIRES].

JHEP11(2009)100